Journal of Ceramic Processing Research. Vol. 3, No. 3, pp. 141~145 (2002)

JOURNAL OF
Ceramic Processing Research

An efficient numerical method for incorporating phase changes in ceramic drying process

Y.T. Keum* and K.H. Auh
Ceramic Processing Research Center (CPRC), Hanyang University, Seoul 133-791, Korea

The numerical simulation of ceramic drying process is difficult as the heat and moisture movements in green ceramics caused by temperature gradients, moisture gradients, conduction, convection and evaporation should be considered. In the finite element formulation for solving temperature and moisture distributions during the drying process, the internally discontinuous interface elements are employed to avoid the numerical divergence problem arising from sudden changes in heat capacity in phase zones. In order to show the reliability of the numerical method proposed in this study, the drying process of a ceramic electric insulator is simulated and the results are compared with those of other investigators.

Key words: Phase Change, Internally Discontinuous Element, Ceramic Drying Process, Ceramic Electric Insulator, Finite Element Method.

Introduction

Computer-aided numerical methods like FEM, FDM, and BEM are widely used to evaluate mechanical characteristics as well as to optimize processing variables. Using the numerical methods, the mechanical characteristics of ceramics affected by temperature and moisture movements in the drying process can be easily evaluated.

Variations of temperature and moisture in the drying process change the volume and induce the hygro-thermal stress. The heat and moisture transfer and the associated hygro-thermal stress are fundamental issues in heat-moisture-stress problems. However, in finding temperature profile and moisture distribution in green ceramics during the drying process using FEM, the numerical divergence problem cannot be avoided due to the changes in material properties in the dual phase area.

The interrelation between heat and moisture transfer in porous materials was established by Luikov who proposed a two-term relationship for the non-isothermal moisture diffusion. The development of the theory of transport phenomena in porous media has been summarized by Luikov [1-3] and Whitaker [4]. The effects of the liquid and vapor transport, heat transport, pressure gradient, and capillary flow were investigated by De Vries *et al*. [5, 6] and a set of coupled diffusion equations of temperature and moisture contents was proposed. Whitaker [4] analyzed the heat, mass, and momentum in porous media and Comini *et al*. [7] performed numerical analysis of the two-dimensional problem involving heat and mass transfer. The validity of this methodology in timber was verified by Thomas *et al*. [8] through the comparison of experimental and numerical results. Dhatt *et al*. [9] modeled a concrete drying process and Gong *et al*. [10] used the finite element method in the concrete drying process and investigated heat transfer velocity and moisture reduction velocity. The stress distribution caused by heat and moisture transfer was analyzed by Lewis *et al*. [11] using the finite element method in the drying process of a brick, a ceramic electric insulator, and a basement foundation. The hygro-thermal stress caused by heat and moisture transfer in composite materials was also analyzed by Sih *et al*. [12].

In this study, a numerical method solving the two-phase problem in the finite element analysis for temperature and moisture distributions during the drying process of ceramics is introduced. For the verification of the numerical approach, the drying process of a ceramic electric insulator is simulated.

Finite Element Formulation

The rate of temperature and moisture transfer in a body is caused by their flux gradients as well as source rates [1-3]:

$$C\frac{\partial T}{\partial t} = -\nabla\cdot\mathbf{j_q} + \dot{I}_q = \nabla\cdot(\mathbf{K^M}\cdot\nabla W + \mathbf{K^T}\cdot\nabla T) + \dot{I}_q \qquad (1)$$

$$\frac{\partial W}{\partial t} = -\nabla\cdot\mathbf{j_m} = \nabla\cdot(\mathbf{A^M}\cdot\nabla W + \mathbf{A^T}\cdot\nabla T + \mathbf{A^g}\cdot W\mathbf{g}) \qquad (2)$$

where T is temperature, W is the moisture, C is the

*Corresponding author:
Tel : +82-2-2290-0436
Fax: +82-2-2298-6194
E-mail: ytkeum@hanyang.ac.kr

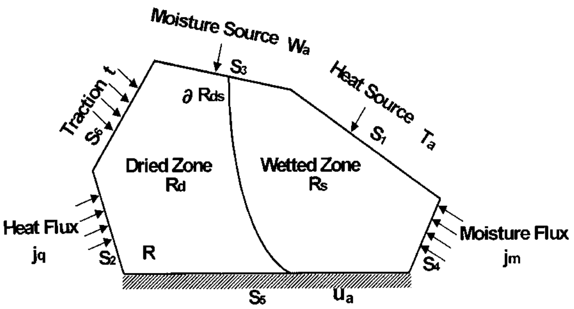

Fig. 1. Schematic view of heat and moisture transfer problem.

bulk specific heat per unit volume, $\mathbf{j_q}$ is the heat flux vector, $\mathbf{j_m}$ is the moisture flux vector, i_q is the heat source function, $\mathbf{K^M}$ is the diffusion-thermal coefficient tensor, $\mathbf{K^T}$ is the heat conductivity tensor, $\mathbf{A^M}$ is the moisture diffusivity tensor, $\mathbf{A^T}$ is the thermal diffusion coefficient tensor, and $\mathbf{A^g}$ is the forced flux coefficient tensor. Figure 1 is a schematic diagram of the heat and moisture transfer problem. During the drying process of a ceramic product, the flux and source of heat and moisture as well as traction are respectively subjected to simultaneously existing dried and wetted zones in the ceramic body. The problem definition provides the boundary conditions expressed as follows:

$$T=T_a \text{ on } S_1 \tag{3}$$

$$k_q\nabla T\mathbf{n}+\mathbf{j_q}+\alpha_\mathbf{q}(T-T_a)+(1-\varepsilon)\alpha_\mathbf{m}\lambda(W-W_a)=0 \text{ on } S_2 \tag{4}$$

$$W=W_a \text{ on } S_3 \tag{5}$$

$$k_m\nabla W\mathbf{n}+\mathbf{j}_m+k_m\delta\nabla T\mathbf{n}+\alpha_m(W-W_a)=0 \text{ on } S_4 \tag{6}$$

$$S_1YS_2=\partial R \tag{7}$$

$$S_3YS_4=\partial R \tag{8}$$

where T_a is a prescribed temperature on the boundary S_1, $\mathbf{j_q}$ is heat flux on the boundary S_2, W_a is a prescribed moisture on the boundary S_3, $\mathbf{j_m}$ is moisture flux on the boundary S_4, k_q is a thermal conductivity, k_m is moisture conductivity, $\mathbf{n}$ is an outward normal vector on the surface of the boundary, α_q is a convective heat transfer coefficient, α_m is a convective moisture transfer coefficient, [?]ε is a ratio of the vapor diffusion coefficient to the total diffusion coefficient of moisture, **[?]**λ is a heat of phase change, **[?]**δ is a thermo-gradient coefficient, and ∂R is a boundary of control volume R. Eq. (3) and Eq. (5) represent boundary conditions on the portion of the material boundary where constant temperature and constant moisture are prescribed, respectively. Eq. (4) and Eq. (6) also represent those portions on the boundary subjected to heat and moisture flux. Eq. (4) and Eq. (6) can be rewritten in the compact form as follows:

$$k_q\nabla T\mathbf{n}+\mathbf{j}_q^*=0 \text{ on } S_2 \tag{9}$$

$$k_m\nabla W\mathbf{n}+\mathbf{j}_m^*=0 \text{ on } S_4 \tag{10}$$

where

$$\mathbf{j_q^*}=\mathbf{A_q}(T-T_a)+\mathbf{A}_\varepsilon(W-W_a)+\mathbf{j_q} \tag{11}$$

$$\mathbf{j_m^*}=\mathbf{A}_\delta(T-T_a)+\mathbf{A_m}(W-W_a)+\mathbf{j_m}-\frac{k_m\delta}{k_q}\mathbf{j_q} \tag{12}$$

$$\mathbf{A_q}=\alpha_q \tag{13}$$

$$\mathbf{A}_\varepsilon=(1-\varepsilon)\alpha_m\lambda \tag{14}$$

$$\mathbf{A}_\delta=-\frac{k_m\delta\alpha_q}{k_q} \tag{15}$$

$$A_m=\alpha_m-\frac{(1-\varepsilon)\alpha_m k_m\lambda\delta}{k_q} \tag{16}$$

At the evaporation temperature during the heat and moisture transfer, a phase change phenomenon occurs such that the moisture within the material is liquefied or vaporized and two phases exist simultaneously. To analyze effectively the heat and moisture moving boundary problem during the phase transition process in an element, energy conservation is considered. A schematic view of the heat and moisture moving boundary problem in the interface between the dried and wetted zones is shown in Fig. 2. As the latent heat of evaporation in the interface is due to the difference in heat flux between the dried and wetted zones, the energy conservation equation in the interface between the dried zone and the wetted zone can be written as follows:

$$L(W_0\dot{\mathbf{X}}+\mathbf{j_m})\cdot\mathbf{n_{ds}}=(\mathbf{j_{qd}}-\mathbf{j_{qs}})\cdot\mathbf{n_{ds}} \tag{17}$$

where L is the latent heat of evaporation, W_0 is the resident moisture content, $\mathbf{X}$ is the position of the interface, $\mathbf{n_{ds}}$ is a unit normal vector in phase change zone, $\mathbf{j_{qd}}$ is a heat flux vector in dried zone, and $\mathbf{j_{qs}}$ is a heat flux vector in the wetted zone.

Defining the temperature T, moisture W, temperature gradient ∇T, and moisture gradient ∇W in a finite element as follows:

$$T=\langle N\rangle\{T\} \tag{18}$$

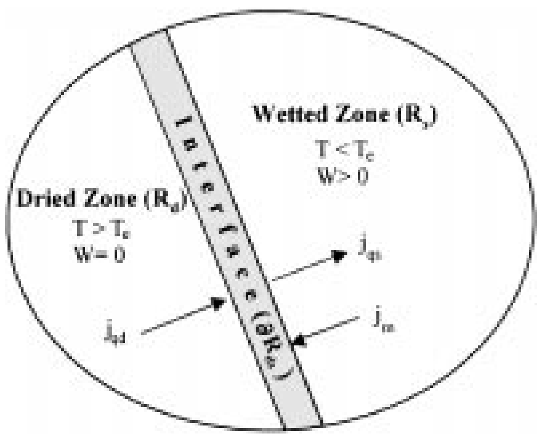

Fig. 2. Schematic view of heat and moisture moving boundary problem in the interface.

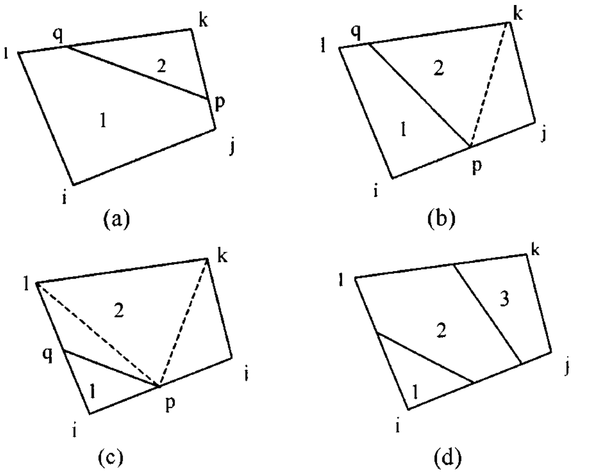

Fig. 3. Internally discontinuous, isoparametric elements. (1or 3 for dried or wetted zone, 2 for phase transition zone).

$$W=\langle N\rangle\{W\} \tag{19}$$

$$\nabla T=[B]\{T\} \tag{20}$$

$$\nabla W=[B]\{T\} \tag{21}$$

where <N> denotes an appropriate shape function, {T} is a nodal temperature vector, {W} is a nodal moisture vector, and [B] is a differential matrix of shape function, the finite element equations can be expressed as follows:

$$\sum_{e=1}^{E}\left(\begin{bmatrix} C^T & 0 \\ 0 & C^M \end{bmatrix}\begin{Bmatrix} \dot{T} \\ \dot{W} \end{Bmatrix}+\begin{bmatrix} K^{TT} & K^{TM} \\ K^{MT} & K^{MM} \end{bmatrix}\begin{Bmatrix} T \\ W \end{Bmatrix}-\begin{Bmatrix} F^T \\ F^M \end{Bmatrix}\right)_e=0 \tag{22}$$

where the matrices including the conductivity terms C^T and C^M, the stiffness terms K^{TT}, K^{TM}, K^{MT} and K^{MM}, and the force terms F^T and F^M are called heat capacity matrix, stiffness matrix and force vector, respectively.

If there exists two phases in a finite element, the numerical divergence happens because of the change in material properties, especially heat capacity. To avoid this problem, internally discontinuous, isoparametric elements [13] are introduced as shown in Fig. 3. There are 4 sorts of elements according to the state of phases in an element. Because the change in temperature in the quadrilateral element is assumed to be linear, the interface can be expressed as a straight line across the element. When the interface passes through the element sides at p and q, as shown in Fig. 3(a), the x-coordinates of point p and point q are respectively calculated as follows:

$$x_p=x_j+\frac{T_{12}-T_j}{T_k-T_j}(x_k-x_j) \tag{23}$$

$$x_q=x_k+\frac{T_{12}-T_k}{T_l-T_k}(x_l-x_k) \tag{24}$$

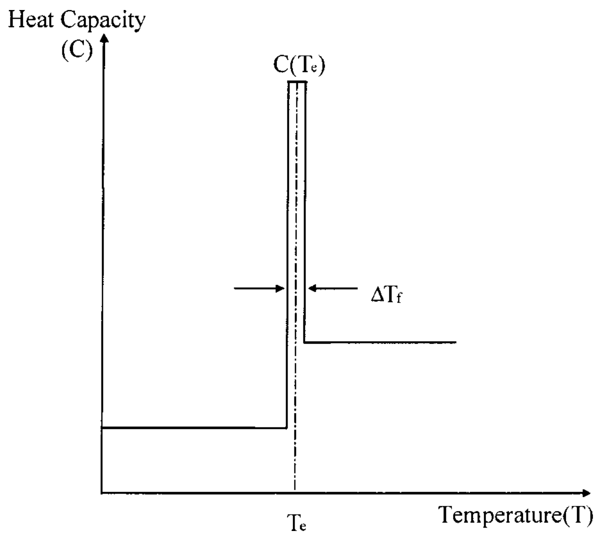

Fig. 4. Heat capacity(C) at phase transition temperature (T_e).

where $T_e-0.5\Delta T_f \leq T_{12} \leq T_e+0.5\Delta T_f$ is the transition temperature separating zone 1 and zone 2, T_e is the phase transition temperature, and ΔT_f is the temperature width of the phase transition zone, as shown in Fig. 4. In a similar fashion, equations such as Eq. (23) and Eq. (24) can be used to find the y-coordinates of point p and point q, y_p and y_q, respectively.

The heat capacity in the discontinuous element can be computed by superimposing the difference in heat capacity of different zones as follows:

$$C^T=\int_R \{N\}C_1\langle N\rangle dR+\int_{R_2}\{N\}\Delta C_{12}\langle N\rangle dR \tag{25}$$

where R_2 is a region of zone 2 and $DC_{12}=C_2-C_1$ is the difference in heat capacity between zone 1 and zone 2 as seen in Fig. 3(a). The second term in Eq. (25) can be changed at the centroid (x_r, y_r) of zone 2 as follows:

$$\int_{R_2}\{N\}\Delta C_{12}\langle N\rangle dR=\Delta C_{12}A_{R_2}\begin{bmatrix} N_1^2 & & 0 \\ & N_1^2 & \\ & & \cdot \\ 0 & & \cdot \end{bmatrix}_{(s_r,t_r)} \tag{26}$$

where AR2 is the area of R2 and (sr, tr) is the coordinate of a centroid of the isoparametric element. When R2 is a quadrilateral or pentagon, it is divided into two or three triangles as shown in Fig. 3(b) and Fig. 3(c) to find the heat capacity by the same procedure as that in Fig. 3(a).

When the width of a phase transition zone is very narrow, the phase transition zone can be shown as in Fig. 3(d). In this case, the heat capacity can be obtained in a similar manner as Eq. (25) as follows:

$$C^T=\int_R \{N\}C_1\langle N\rangle dR+\int_{R_2+R_3}\{N\}\Delta C_{12}\langle N\rangle dR$$

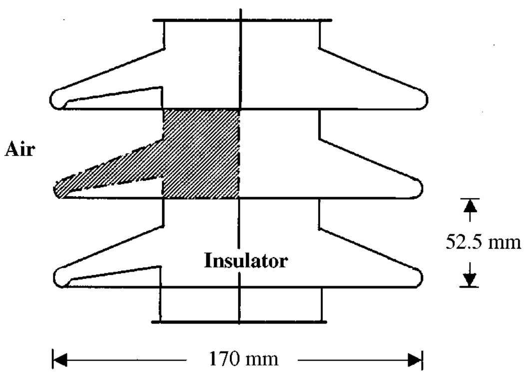

Fig. 5. Schematic view of a ceramic electric insulator.

$$+\int_{R_3} \{N\}\Delta C_{23}\langle N\rangle dR \qquad (27)$$

If **jm** is a constant in a discontinuous element, the evaporation energy of inflow liquid is computed as follows:

$$\mathbf{j}_{\mathbf{m}} = -(\mathbf{A}^{\mathbf{M}}\cdot\nabla W + \mathbf{A}^{\mathbf{T}}\cdot\nabla T + \mathbf{A}^{\mathbf{g}}\cdot W\mathbf{g}) \\ -(\mathbf{A}^{\mathbf{M}}[B]\{W\} + \mathbf{A}^{\mathbf{T}}[B]\{T\} + \mathbf{A}^{\mathbf{g}}\cdot g\langle N\rangle\{W\}) \qquad (28)$$

Numerical Verification

In order to show the validity of the proposed numerical method, the drying process of a ceramic electric insulator is simulated. A schematic view of a ceramic electric insulator is illustrated in Fig. 5. The hatched area is modeled for the simulation due to the symmetry. In the finite element model, 290 nodes and 248 quadrilateral linear elements are employed. The green insulator initially lies in a state of constant 25°C temperature and 80 kg/m^3 moisture. The ambient temperature and moisture are 60°C and 40 kg/m^3, respectively. Adiabatic and symmetric conditions are imposed on three sides except the boundary exposed to the air. As time elapses, the heat and moisture transfer from the boundary to the interior.

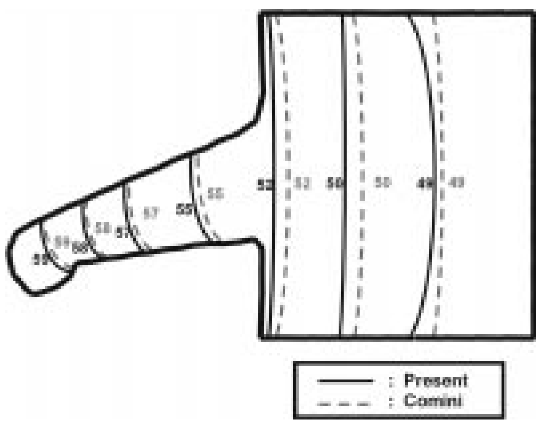

Fig. 6. Comparison of temperature distribution in ceramic electric insulator between Comini and present results.

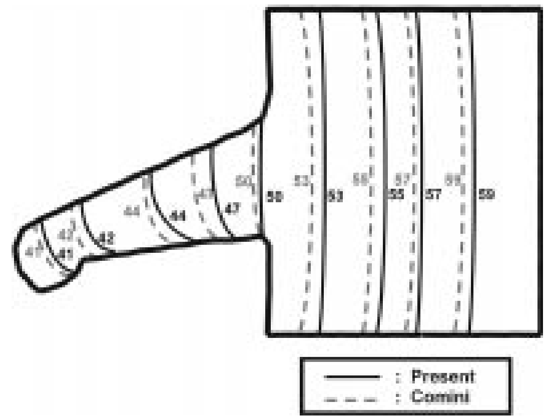

Fig. 7. Comparison of moisture distribution in ceramic electric insulator between Comini and present results.

Figure 6 and Fig. 7 show temperature and moisture distributions after drying 5 hours. The present results, shown as solid lines, are similar to Comini's analysis [11], shown with dotted lines. As time goes on, it is supposed that the hygro-thermal stress should be larger because of the big temperature and moisture gradients.

Conclusion

For the finite element simulation to find temperature and moisture distributions in the ceramic drying process, a numerical approach to solve a dual phase problem is introduced. To verify the proposed numerical method, the drying process of a ceramic electric insulator is simulated. Through this study, the internally discontinuous elements are suggested to efficiently describe a phase change phenomenon in the drying process.

Acknowledgements

This work was supported by the Korea Science and Engineering Foundation (KOSEF) through the Ceramic Processing Research Center at Hanyang University.

References

1. Luikov, A.V., “Systems of Differential Equations of Heat and Mass Transfer in Capillary-Porous Bodies (Review)”, Int. J. Heat Mass Transfer. Vol. 18 (1975) 1-14.
2. Luikov, A.V., Heat and Mass Transfer in Capillary-Porous Bodies, Pergamon, Oxford (1975).
3. Luikov, A.V., Heat and Mass Transfer, Mir Publishers, Moscow (1980).
4. Whitaker, S., “Simultaneous Heat, Mass and Momentum Transfer in Porous Media: A Theory of Drying”, Advances in Heat Transf. Vol. 13 (1977) 119-203.
5. De Vris, D.A., “Simultaneous Transfer of Heat and Moisture in Porous Media”, Trans. Am. Geophys. Un. Vol. 39 No. 5 (1958) 909-916.
6. Philip, J.R. and De Vris, D.A., “Moisture Movement In

Porous Materials under Temperature Gradients", Trans. Am. Geophys. Un. Vol. 38 No. 2 (1957) 222-232.

7. Comini, G. and Lewis, R.W., "A Numerical Solution of Two-Dimensional Problem Involving Heat and Mass Transfer", Int. J. Heat Mass Transfer. Vol. 19 (1976) 1387-1392.
8. Thomas, H.R., Lewis, R.W. and Morgan, K., "An Application of The Finite Element Method to The Drying of Timber", Wood Fibre. Vol. 11 (1980) 237-243.
9. Dhatt, G., Jacquemier, M. and Kadje, C., "Modelling of Drying Refractory Concrete", Drying '86. No. 1 (1986) 94-104.
10. Gong, Z.X. and Mujumdar, A.S., "Development of Drying Schedules for One-Heating Drying Refractory Concrete Slabs Based on A Finite Element Model", J. Am. Ceram. Soc. Vol. 79 No. 6. (1969) 1649-1658.
11. Lewis, R.W., Strada, M. and Comini, G., "Drying-Induced Stressed in Porous Bodies", Int. J. Num. Meth. Engng. Vol. 11 (1977) 1175-1184.
12. Sih, G.C., Ogawa, A. and Chou, S.C., "Two-Dimensional Transient Hygrothermal Stresses in Bodies with Circular Cavities: Moisture and Temperature Coupling Effects", J. Thermal Stresses. Vol. 4 (1981) 193-222.
13. Steven, G.P., "Internally Discontinuous Element for Moving Interface Problems", Int. J. Num. Meth. Engng. Vol. 18 (1982) 569-582.